JGR Biogeosciences

RESEARCH ARTICLE
10.1029/2021JG006714

Gradient Studies Reveal the True Drivers of Extreme Life in the Atacama Desert

D. Boy[1,2], R. Moeller[3], L. Sauheitl[2], F. Schaarschmidt[4], S. Rapp[5], L. van den Brink[6], S. Gschwendtner[7], R. Godoy Borquez[8], Francisco J. Matus[9,10], M. A. Horn[1], G. Guggenberger[2], and J. Boy[2]

[1]Institute of Microbiology, Leibniz Universität Hannover, Hannover, Germany, [2]Institute of Soil Science, Leibniz Universität Hannover, Hannover, Germany, [3]German Aerospace Center (DLR), Institute of Aerospace Medicine, Radiation Biology Department, Aerospace Microbiology Research Group, Cologne, Germany, [4]Institute of Cell Biology and Biophysics, Leibniz Universität Hannover, Hannover, Germany, [5]Dastani Consulting GmbH, Wettenberg, Germany, [6]Institute of Evolution and Ecology, University of Tubingen, Tübingen, Germany, [7]Helmholtz Zentrum München, COMI Research Unit Comparative Microbiome Analysis, Neuherberg, Germany, [8]Instituto de Ciencias Ambientales y Evolutivas, Universidad Austral de Chile, Valdivia, Chile, [9]Laboratory of Conservation and Dynamics of Volcanic Soils, Department of Chemical Sciences and Natural Resources, Universidad de La Frontera, Temuco, Chile, [10]Network for Extreme Environmental Research (NEXER), Universidad de La Frontera, Temuco, Chile

Key Points:

- Gradient studies are more suitable to elucidate the boundaries of habitability of extreme habitats as compared to non-gradual studies
- At the Atacama, transects perpendicular to the Andes displayed multiple drivers of aridity while gradients parallel were much less biased
- Honest analogue research has to clearly allot the contribution of external sources, which otherwise results in questionable conclusions

Supporting Information:

Supporting Information may be found in the online version of this article.

Correspondence to:

D. Boy,
diana.boy@ifmb.uni-hannover.de

Citation:

Boy, D., Moeller, R., Sauheitl, L., Schaarschmidt, F., Rapp, S., Brink, L., et al. (2022). Gradient studies reveal the true drivers of extreme life in the Atacama Desert. *Journal of Geophysical Research: Biogeosciences*, *127*, e2021JG006714. https://doi.org/10.1029/2021JG006714

Received 10 NOV 2021
Accepted 7 FEB 2022

Author Contributions:

Conceptualization: D. Boy, R. Moeller, R. Godoy Borquez, G. Guggenberger, J. Boy
Data curation: D. Boy
Formal analysis: D. Boy, F. Schaarschmidt, S. Rapp, J. Boy
Funding acquisition: R. Godoy Borquez, Francisco J. Matus, G. Guggenberger, J. Boy
Investigation: D. Boy, L. Sauheitl, L. van den Brink, J. Boy
Methodology: D. Boy, R. Moeller, L. Sauheitl, F. Schaarschmidt, S. Rapp, S. Gschwendtner, M. A. Horn, J. Boy

Abstract Studies of hyper-arid sites contribute to our understanding on how life adapted to extreme conditions. They are often used to further deduce implications for extraterrestrial biology by the so-called analogue site-approach. The Atacama Desert, Chile, is one of the most prominent analogue sites despite its neighboring productive ecosystems due to its hyper-aridity and geochemical features resembling Martian environments. We hypothesize that many drivers of extremophile life in analogue sites are only mistakenly attributed to aridity alone, thus obscuring a clear view of the far more complex process interactions originating in nearby earthly ecosystems. To test this, we investigated 54 soil profiles up to 60 cm of soil depth along of four transects in the Atacama Desert, either running parallel (S-N) or perpendicular (W-E) to the Andes. Our objective was to reveal the processes controlling the formation of soil organic carbon (SOC) as the most reliable proxy for microbial life in order to understand the boundary conditions of life in extreme habitats. Further, we aimed at identifying analogue sites as uncompromised as possible by external influences of for example, vegetated or marine ecosystems. We found a mixture of influences driving habitable conditions on gradients perpendicular to the Andes, for example, fog and precipitation scavenging caused by altitudinal variations and differing proximity to the Pacific Ocean, while transects parallel to the Andes were much less biased by external factors. Our results show that studies on life under extreme conditions should clarify the explanatory strength of the investigated factors by a gradient study approach.

Plain Language Summary Being the driest desert on Earth, the Atacama Desert is often regarded as resembling the living conditions on Mars making it a so-called analogue site. Analogue sites are used to learn about the boundary conditions of microbial life and also help at understanding the evolution of life. The Atacama Desert is a hyperarid place alike Martian environments, but is influenced by factors clearly not occurring on Mars, for example, a highly productive Ocean nearby. Thus, if one wants to learn about the effects of aridity on the microbial life alone, an exclusion of other gradual influences is necessary. We aimed at identifying genuine aridity gradients and distinguishing them from gradients influenced by multiple drivers. We found that parallel to the Andes, a true climatic gradient with precipitation being the only changing parameter exists, while perpendicularly directed gradients displayed a mixture of influences. Future research on life along aridity gradients in the Atacama are most promising in the Longitudinal Valley to ensure a genuine climatic gradient. With this study, we hope to disentangle the multiple drivers which could be misleadingly interpreted as aridity features and highlight the chances of gradient approaches to ensure fair conclusions about driving factors in extreme environments.

1. Introduction

Analogue studies, which use extreme conditions on earth to draw conclusions for life elsewhere in the universe, seem often to be shortened to the assumption, that hyper-aridity alone determines an for example, Mars-like

Project Administration: D. Boy, R. Godoy Borquez, G. Guggenberger, J. Boy
Resources: D. Boy, R. Moeller, L. Sauheitl, S. Gschwendtner, Francisco J. Matus, M. A. Horn, J. Boy
Software: D. Boy, F. Schaarschmidt, S. Rapp
Supervision: R. Moeller, G. Guggenberger, J. Boy
Validation: L. Sauheitl, M. A. Horn, G. Guggenberger, J. Boy
Visualization: D. Boy, L. van den Brink
Writing – original draft: D. Boy
Writing – review & editing: D. Boy, R. Moeller, L. Sauheitl, F. Schaarschmidt, S. Rapp, L. van den Brink, S. Gschwendtner, R. Godoy Borquez, Francisco J. Matus, M. A. Horn, G. Guggenberger, J. Boy

environment, while forgetting about the close proximity of highly productive ecosystems which are not Mars-like at all (Connon et al., 2007). These neighbor ecosystems are biogeochemically connected to these putative extreme environments, for example, by potentially receiving aeolian deposition of SOC or salts and air humidity. Without tracking the extent of these influences along gradients toward the hyper-arid cores of deserts, their role on habitability and microbial community composition stays unclear. The properties and functioning of soils are thereby impacted by environmental gradients and controlled by long-lasting effects of local biotic and abiotic conditions such as climate, geology, geomorphology, and living organisms interacting with their soil environment (Galun, 2019; Gillison & Brewer, 1985; Siqueira et al., 2021). Soils are extraordinarily heterogeneous dynamic systems complicating the transfer of gained results onto soils in similar environments for the purpose of process analysis or prediction. Nevertheless, space-for-time or space-for-climate substitution are widespread tools in ecosystem research, although separation of driving factors is complicated and still a matter of scientific debate (Liu et al., 2018; Metz et al., 2015; Tielbörger et al., 2014).

An example of the difficulties in disentangling driving factors along transects are aridity gradients into deserts. While the initial disappearance of vegetation is easy to observe, optical uniformity thereafter complicates a direct identification of the driving parameters of life. The picture is further blurred by interconnected parameters like precipitation and altitude which potentially alter the expected climatic conditions. Thus, a thorough understanding of the specific sites that is, the knowledge about existing on-site gradients, prior to field sampling is crucial to later understand the underlying processes of any gradient.

In detail, analogue studies as one of the varieties of desert studies observe the adaptation and niching strategies of microbial communities in their natural habitat. The aim of those studies is to deviate the potential of detecting biosignatures from abiotically and geochemically similar terrestrial sites and to gain insights on potential habitats for live on other planets (Billi et al., 2019; Cortesão et al., 2019; Knief et al., 2020). Thus, certain traits of terrestrial analogue sites are believed to help to reveal processes which might have been crucial for the support of life on early Mars (García-Descalzo et al., 2019; Warren-Rhodes et al., 2019). However, finding analogue sites on Earth for all the different environments, which exist on Mars, is challenging because of their number and diversity. During the drying-out of Mars (Kite et al., 2019) soils were assumedly subject to similar processes found today in the driest deserts on Earth (Sutter et al., 2007). As a consequence, Martian regolith may be as heterogeneous as the soils in terrestrial deserts which stresses the need of a proper experimental design for the exploration of any suitable analogue site. Transect studies offer the possibility to disentangle the otherwise confounding parameters that control the boundary conditions of habitability.

Due to its extreme and long-lasting aridity (precipitation <2 mm yr^{-1}) and several geochemical features resembling Martian conditions, the hyper-arid core of the Atacama Desert between 15° and 30°S is ideal for analogue studies (Houston & Hartley, 2003; McKay et al., 2004). Several abiotic traits influencing the occurrence of life in the Atacama Desert should be considered before choosing analogue sampling sites and setting up experiments. The altitude of the Atacama ranges from 0 to >6000 m above sea level (a.s.l.) with several mountain ranges and valleys between the Coastal Cordillera to the Andes Cordillera generating diverse and discrete climatic conditions ranging from permafrost to hot and from semi-arid to hyper-arid conditions (Hartley et al., 2005; Nagy et al., 2019; Sun et al., 2018). A dense coastal fog from the Pacific Ocean called Camanchaca penetrates the coastal cordillera up to 90 km inland with humidity feeding the coast line (Rech et al., 2003). Thus, precipitation decreases from the West to the East of the Central Valley, creating distinct reliefs, which are responsible for the huge longitudinal heterogeneity (Houston, 2006), but which have also some common features: An often steeply inclined Coastal Cordillera in the west is followed by the flat, crust-rich Central valley that contrasts the ridges of the Cordillera Domeyko, while the highest summits are reached in the Cordillera de los Andes to the east (Clarke, 2006). The relief and inclination lead to many small-scale modulations of potential habitable niches, as they for example, change microclimatic conditions, accumulate soils at the toe-slopes of hills, channel temporary water flow events into gullies, or affect soil temperatures due to the diurnal course of shading (Barry, 1992; Casanova et al., 2013; Ran et al., 2012). All these traits contribute to the Atacama Desert being a place with all kinds of sharp gradients on differing scales. Thus, the decision for a sampling site is likely determined by how these gradients and their driving forces fit to the desired research question.

In fact, the right choice of the environmental predictors is one of the major challenges in ecological modeling, as they affect the outcome of the applied models (Araújo & Guisan, 2006; Austin & van Niel, 2011), thus selecting the specific response variables remains difficult. For studies dealing with aridity gradients, several soil

parameters serve as suitable indicators for habitability. The availability of water, measured as soil water content (SWC), influences the occurrence of life either as a premise for photosynthesis and metabolic activity or as a solvent for nutrients (Liu et al., 2018). Soil organic carbon (SOC) can exclusively be produced by living organisms, thus it delivers hints about the productivity of autotrophic communities, the turn-over, and mineralization processes of heterotrophic organisms (Azua-Bustos et al., 2019) and it correlates well with microbial abundances (Knief et al., 2020).

A major limitation of life in deserts are imposed by salt accumulations. Salts in the soil can become quite counterintuitively as they either inhibit the occurrence of non-adapted microbes by creating an osmotically active environment (Zhang et al., 2019), or enable life to halophilic species (Azua-Bustos et al., 2018) due to deliquescence (Davila et al., 2013; Shen et al., 2021). Deliquescence is the process of phase transition from solid, crystallized salts into a liquid, salty solution induced by highly saturated air humidity (Gómez-Silva, 2018; Uritskiy et al., 2019). Soluble salts are transported to the Atacama where they precipitate and accumulate in soils due to high evaporation (Ewing et al., 2006). Nitrates derive from marine sources, radiation-induced photodegradation, and biologic nitrification in the Atacama (Ewing et al., 2006; Galloway et al., 2004; Michalski et al., 2004), while sulphates and calcium are either released from rock weathering, or deposited after aeolian transport from marine or volcanic sources (Finstad et al., 2016; Rech et al., 2003).

Soil texture, a consequence of weathering and geology, may be of interest in analogue research because of its possibility to deduce nutrient supply from the minerals involved providing exchange and water retention capacity. Deeply weathered soils are often a consequence of intense biogenic weathering (Brantley et al., 2011; Taylor et al., 2009), nourishing the hope to find traces of life. Changes in soil texture are not controlled by climatic conditions alone, but bed rock composition and biotic interactions also play their role. Soil texture possibly serves as an indicator for the heterogeneity of a study site rather than being subject to a gradual shift.

Despite the advantages of the gradient approach for analogue studies, also different approaches have been employed in the Atacama. Roughly half of the studies used a single sampling design, which means that their sampling sites were not chosen to follow a pre-defined transect. Instead those sites were chosen to fulfil the requirement of being situated in a certain salar, lagoon or consisting of a specific substrate, for example, halite, gypsum (e.g., Davila et al., 2008; Finstad et al., 2016). The other half of the studies opted for a transect-based set-up, either following altitude or aridity or both (e.g., Burgener et al., 2016; Crits-Christoph et al., 2013; Diaz et al., 2016). Thereby, gradients following aridity (South to North, West to East or West to Southeast) with or without altitudinal changes showed a grand band width of possible locations in the Atacama Desert.

Taking all the described circumstances, the question arises if this plethora of variability and options really helps the case of analogue studies. Therefore, the aim of this study is to evaluate the process interactions determining habitability in hyper-arid analogue sites along contrasting gradients in the Atacama Desert by comparing the two most common transect directions parallel (South-North) and perpendicularly (West-East) to the Ocean and the Andes. We define SOC content as our measure for habitability, as it is only produced by life itself and correlates with DNA content in Atacaman soils (Figure S2 in Supporting Information S1). In a modelling approach we aim to clarify to which extent climatic and edaphic factors determine the content of SOC, thus habitability. Further, we evaluate whether these drivers are related to aridity alone or rather represent a mixture of other driving factors mimicking Mars-like conditions but in fact being created by very earth-like influences. Here, we hypothesize that analogue studies as well as any study on extreme environments require a process-oriented and gradient-based understanding of their respective habitability to disentangle the mixture of driving patterns, enabling comparability, recovery and up-scalability of results. In this regard, we hypothesise that many drivers of extremophile life in deserts are only mistakenly attributed to aridity alone, thus obscuring a clear view of the far more complex process interactions.

2. Materials and Methods

2.1. Study Sites

For the preselection of the transect directions we oriented ourselves on the available literature summarized in Table 1. In parallel, satellite imagery with Google Earth Pro was used and climate and weather data derived via the geographic information system QGIS Version 2.18.13. Climatic data revealed that due to size, topography

Table 1
Overview of the Different Experimental Designs and Gradients Published by Other Authors in the Atacama Desert

Location	Set-up	No. of sites	Type of samples	Interest	Reference
Salar de Llamara	Single sampling	2	Soil	Evaporation	Finstad et al., 2016
Yungay	Single sampling	3	Lagoon water	Microbial diversity	Azua-Bustos et al., 2018
Valle de la Luna & Monturaqui	Single sampling	2	Different lithic substrates	Microbial diversity	Meslier et al., 2018
Yungay	Single sampling	2	Soil	Microbial diversity	Connon et al., 2007
Pacific Ocean	Single sampling	1	12 m sediment core	Rainy past of the Atacama	Contreras et al., 2010
Yungay	Single & time sampling	1	Air & crust	Halite deliquescence	Davila et al., 2008
Yungay	Single sampling	1	Soil	Rain infiltration	Davis et al., 2010
Atacama, Mojave, & al-Jafr Basin	Single sampling	3	Soil gypsum	Cyanobacteria	Dong et al., 2007
Salar de Atacama	Random sampling	7	Water & soil	Origin of solutes	Carmona et al., 2000
Salar de Llamara	W-SE aridity gradient	3	Halite crust	Microbial diversity	Finstad et al., 2017
Iquique & Tocopilla	WE & time	3 each	Viable bacteria	Aeolian transport	Azua-Bustos et al., 2019
Ojos del Salado	Altitudinal	4	Sediment	Microbial diversity	Aszalós et al., 2016
Valle del Elqui	Altitudinal	20	Water & soil	Carbonate formation	Burgener et al., 2016
Chanaral to Yungay	S-N	4	Soil	Microbial diversity	Crits-Christoph et al., 2013
Salars & lagunes	Altitude, salinity & UV	19	Water	Microbial diversity	Demergasso et al., 2006
East of Salar de Atacama	Altitude, temperature & aridity	20	Soil, plants, feces	N-cycle	Diaz et al., 2016
Antofagasta to Volcán de Llullaico	Altitude & aridity	12	Soil	Microbial diversity	Drees & Neilson, 2006
Copiapo/Altamira & Yungay	S-N	3	Soil	Soil formation	Ewing et al., 2006
Nahuelbuta to Pan de Azucar	S-N	4	Soil	Weathering & diversity	Oeser et al., 2018
Vallenar to Maria Elena	S-N	7	Soil	Microbial diversity	Shen et al., 2021
Yungay & La Joya Peru	Arbitrary sampling	3	Soil	Variability of SOC	Fletcher et al., 2012

Note. Roughly half of the studies used single sampling, while the rest was at gradient basis.

and location of the Atacama Desert the amount of precipitation is heterogeneously distributed across the desert, dividing it into semiarid, arid, and hyper-arid regimes depending on altitude and geographic location.

During the field campaign, four transects were identified in order to test our hypothesis. We did not select for soil type, as soil development clearly differs along such steep gradients. Seven sites follow a South to North ("SN") transect at constant distance of roughly 40 km to the Pacific Ocean in the Central Valley between the Coastal Cordillera and the pre-Andean Cordillera Domeyko. All sites - sampled roughly every 100 km - are located in a plane and wide deflated landscape without a visible exposition or inclination. Additionally, it was assured that the sites were not located in wadis/aguadas. The GPS coordinates lie between S22.79° and S29.14° and between W69.69° and W70.88° ranging from arid to hyper-arid climatic regimes according to the definition of UNEP (Barrow, 1992). Additionally, a total of 13 sampling sites are located perpendicularly, thus in West-East ("WE") direction on three soil sampling gradients. In the following we call these sampling gradients "sWE" meaning the southerly located West-East transect, "mWE" meaning the middle of the three West-East transects or "nWE" meaning the northerly located West-East transect. The western-most plots of each of the West-East transects are always located close to the Pacific Ocean on the western rim of the Coastal Cordillera. Two of the plots of each transect lie in the central valley and cross one sampling site of the South-North transect, while the eastern-most plots are located in the High Andes. As the four transects form a raster, the three WE-transects can be taken as additional SN gradients of less resolution, if the single plots are combined accordingly (e.g., sWE-1 + mWE-I + nWE-A = S-N transect at the coast).

Their distribution ranges from the Pacific coast to the High Andes on different latitudes between 21°–28°S and 67°–71°W. Figure 1 shows the location of the four transects and Table 2 the GPS coordinates, the direction of the gradients, the mean annual precipitation (MAP) measured between 1970 and 2016 ((CR)2, 2018) the distances

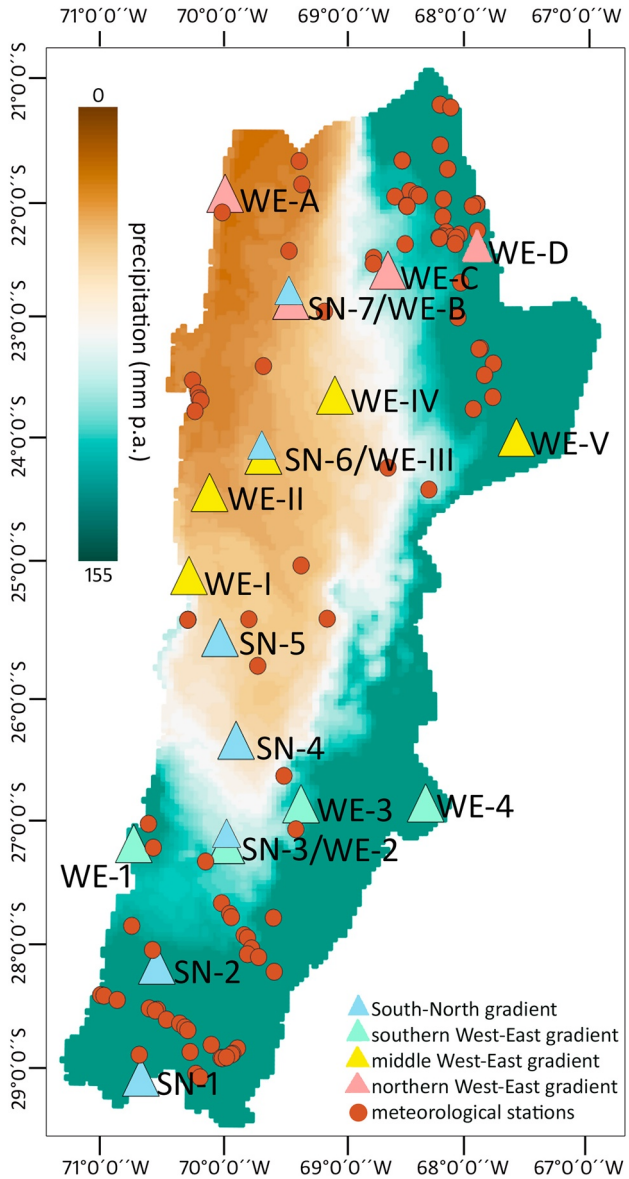

Figure 1. Location of plots in a thematic map showing the mean annual precipitation in mm yr^{-1} and the meteorological stations using QGIS (2017). Data source: Red Cedeus (2021), DGAC (2021), and Arriagada (2016).

from the Pacific Ocean, and the altitude a.s.l. of the plots. The distances from the Pacific Ocean were obtained using Google Earth Pro, Version 7.3.3.7786. Precipitation at the plots sWE-4 in the High Andes and mWE-II on the eastern rim of the Coastal Cordillera were not measured by any meteorological station, thus, were estimated with the missRanger package (Version 2.1.0; Mayer, 2019) using Random Forest predictions in Rstudio version 4.0.3 (October 10, 2020; R Core Team, 2020).

2.2. Field Sampling

At each of the seven SN-sites, three repetitive soil profiles up to 60 cm depth were opened manually in February 2016 (Table 2). The three repetitive soil profiles were placed roughly 20 m apart. In every soil profile five depths (0–1 cm, 5–10 cm, 10–20 cm, 30–40 cm, and 50–60 cm) were sampled at all three sides of each profile and bulked within each depth. Exceptions are plot SN-3 (soil profile 1 up to 60 cm, soil profile 2 and 3 until 20 cm of depth) and SN-4 (soil profile 1 up to 40 cm, soil profile 2 and 3 until 20 cm of depth) because of rigid layers which were impossible to break up manually. The 13 WE-sampling sites were sampled in March 2017. Only one soil profile at each WE plot was sampled down to 60 cm soil depth, while the other profiles were sampled up to 20 cm. These depths are comparable to the transect in South-North direction. All soil samples were sieved in situ through a Retsch sieve with 2 mm mesh size and stored at ambient temperature in sterile bags avoiding atmospheric exchange. Bulk density was sampled for each soil depth in each soil profile by a soil corer of 100 cm^3 volume, avoiding compaction. Soils were classified according to IUSS Working Group World Reference Base (WRB) (2015).

2.3. Analyses of Chemical and Physical Soil Properties

To test the hypothesis that many variables can influence SOC, not only aridity, we analyzed the following basic soil parameters as we believe they contribute substantially to our knowledge on aridity gradients.

Soil water content (SWC) was determined gravimetrically by drying soil aliquots for 24 hr at 105°C in a dry cabinet.

Soil organic carbon (SOC) was measured by combustion with an elemental analyzer (Isotope Cube®, Elementar Analysensysteme GmbH, Hanau, Germany linked to an Isoprime Mass Spectrometer®, Isoprime Ltd., Cheadle Hulme, UK). Carbonates, if present, were removed prior to OC measurement with HCl by the acid fumigation method of Harris et al. (2001). Carbon contents per 1 cm of soil were calculated for the different depth increments.

Water-extractable ions of NO_3^-, Cl^-, PO_4^{3-} and SO_4^{2-} were measured via ion chromatography (IC; Dionex ion chromatograph, Thermo Fisher Scientific with DS5 detection stabilizer and CCRS 500 suppressor). To 7 g of <2 mm fine-earth, we added 35 ml of MilliQ water and shook the suspension upside-down for 1 hr to allow the dissolution of ions. Suspensions were centrifuged at 5 min at 739 g and filtered through a <0.45 µm cellulose acetate filter prior to measurement.

For determination of the electric conductivity (EC) and the pH the soil slurries were prepared with a 1:5 volumetric ratio (soil: MilliQ water) as stated before and left for 1 hr to rest. EC was measured in the supernatant using the LF323 Microprocessor Conductivity meter by a Cond 340i WTW, Weilheim, Germany. As the EC strongly depends on the temperature, we standardized all EC values using the suggested correction of 0.019 of the measured EC value per 1°C from the standard temperature of 25°C (Hayashi, 2004). The pH was measured potentiometrically in the same, but freshly stirred suspension using a glass electrode with the Metrohm 632 pH-Meter, Filderstadt, Germany.

Table 2
GPS Coordinates, Altitude, Distance From the Pacific Ocean, and Precipitation for All Plots Along the Four Transects

Plot	Direction	Latitude	Longitude	Altitude (m a.s.l.)	Dist (km)	MAP* (mm yr^{-1})
SN-1	S-N	29°08'13.90"S	70°52'48.00"W	1120	49	52
SN-2	S-N	28°13'19.60"S	70°44'40.30"W	375	43	26
SN-3	S-N	27°14'17.50"S	70°09'17.10"W	894	68	9
SN-4	S-N	26°23'14.10"S	70°04'19.10"W	855	55	8
SN-5	S-N	25°32'53.90"S	70°12'31.00"W	1081	31	6
SN-6	S-N	24°03'35.80"S	69°50'24.10"W	978	67	2*
SN-7	S-N	22°47'48.20"S	69°36'18.50"W	1466	70	2
WE-A	nW-E	21°55'24.00"S	70°09'54.40"W	75	0.58	3
WE-B	nW-E	22°47'48.20"S	69°36'18.50"W	1466	70	2
WE-C	nW-E	22°33'1.30"S	68°46'58.70"W	2565	152	8
WE-D	nW-E	22°54'5.50"S	68°14'14.30"W	2535	213	27
WE-1	sW-E	27°13'50.50"S	70°56'24.70"W	72	0.9	15
WE-2	sW-E	27°14'17.50"S	70°09'17.10"W	894	68	9
WE-3	sW-E	26°54'20.90"S	69°31'14.90"W	2704	127	2.5
WE-4	sW-E	26°53'54.10"S	68°27'46.60"W	4343	231	8
WE-I	mW-E	25°2'34.30"S	70°28'18.10"W	54	0.8	27
WE-II	mW-E	24°21'53.60"S	70°17'49.00"W	2036	24	5
WE-III	mW-E	24°03'35.80"S	69°50'24.10"W	979	68	2*
WE-IV	mW-E	23°34'14.40"S	69°13'58.70"W	1923	120	12
WE-V	mW-E	23°54'49.00"S	67°41'32.20"W	3973	290	32

Note. dist = distance from the Pacific Ocean; MAP = mean annual precipitation; precipitation data obtained from DGAC (2021), (CR)2 (2018), Arriagada (2016), and Red Cedeus (2018). *McKay et al. (2004).

The mass fraction of the different grain sizes for the determination of the clay content was measured according to DIN ISO 11277 via the sedimentation method. Inorganic carbonates and iron oxides were removed prior to the analysis. In case the intended recovery rate of >98% was not achieved, the difference was attributed to the high concentration of soluble salts which were diluted in supernatant and lost during the various washing steps (Table 3: "solublesalts" in % for the loss of salts). Soil texture (clay) is missing for 25 out of 232 samples.

2.4. Statistical Analysis

Boxplots were created using the ggplot2 package (version 3.3.3; Wickham, 2016) in Rstudio (R Core Team, 2020). The barplot was created using SigmaPlot 11.0.0.7 (SigmaPlot, 2008). As all soil variables as well as the geographic variable MAP were strongly right skewed, the data set was log10 transformed to achieve normality. Before performing the log-transformation, small constants have been added to the variables SOC (+0.1), SWC (+0.001), NO_3^- (+1), PO_4^{3-} (+0.01) and solublesalts (+0.01), to deal with measured data values of 0. The size of the constants depend on the range of the measured data. Significance tests were calculated in Rstudio on log10 transformed data with the multcomp package (Version 1.4.17) using one-way ANOVA followed by Tukey's post hoc test for significant differences along the gradients (Bretz et al., 2011). Principal Component Analysis (PCA) were plotted using spectral decomposition to analyze the correlations/covariates between the variables in the packages ggrepel version 0.9.1 and factoextra version 1.0.7 (Alboukadel & Mundt, 2020; Slowikowski, 2021). We applied a mixed-linear effect model on the dataset to reveal those independent predictory variables which have the greatest impact on the SOC content. To account for the hierarchical sampling structure, linear mixed effects models have been run using the variance of the direction of the transects (South-North "SN" or West-East "WE") and the variance between the plots as random effects. Multicollinearity was assessed using variance inflation factor (vif). Due

to collinearity, the predictors altitude (vif = 10) and Cl (vif = 3) were removed before hypotheses tests and parameters estimation of the final model. Fixed effects of the final model were SWC, pH, EC, soluble salts, NO_3^-, PO_4^{3-}, SO_4^{2-}, kmdistancefromPacific, and MAP in mm. These fixed effects were included into the model at the beginning individually to avoid overfitting (Araújo & Guisan, 2006). Later, we added a second non-significant variable to the already significant variables in case they did not correlate (Figure S1 in Supporting Information S1) with the first one to learn which parameters are significant beyond the first one. We also tested for significant parameters using all parameters at the entire dataset and separated later also into the two perpendicular directions (notably, an overfitting could have happened). Parameters were estimated using Restricted Maximum Likelihood (REML). Linear-mixed effect model analysis was performed in the statsmodels package (version 0.5.0) in JupiterLab (version 1.2.6) using Python 3.7.6 at Anaconda Navigator (version 1.9.12; Seabold & Perktold, 2010). We used SOC as an approximation to life, as we found a good correlation of SOC with DNA concentrations of $R^2 = 0.89$ measured in the same samples (Figure S2 in Supporting Information S1) while DNA and SOC were shown to be good estimators for microbial abundance (Knief et al., 2020). Thus, SOC was added as the response variable in the model to elucidate which variables have the greatest effect on the occurrence of signs of life.

3. Results

3.1. Chemical and Physical Soil Characteristics Affected by Aridity

3.1.1. Soil Water Content

Along the SN gradient, SWC decreased significantly tenfold from south to north (Table 3, Table S1). The lowest SWC per sampling depth was observed at plot SN-6 in a depth of 50–60 cm with $1.8{\cdot}10^{-3} \pm 2{\cdot}10^{-4}$ g g^{-1}, highest $0.06 \pm 5.8\ 10^{-4}$ g g^{-1} at plot SN-1 at a depth of 50–60 cm.

Table 3
Measured Soil Parameters per Plot Along Four Different Transects

Plot	pH	EC (µS cm^{-1})	SOC (g m^2)	SWC (g g^{-1})	Cl (mg kg^{-1})	NO_3^- (mg kg^{-1})	PO_4^{3-} (mg kg^{-1})	SO_4^{2-} (mg kg^{-1})	CLAY (%)	Soluble salts* (%)
SN-1	8.0 ± 0.46	772 ± 1173	27.2 ± 12.6	0.030 ± 0.021	1033 ± 1748	62.8 ± 64.9	11.0 ± 10.2	141 ± 266	22.9 ± 10.3	1.71 ± 2.13
SN-2	9.0 ± 0.21	137 ± 107	9.0 ± 3.02	0.007 ± 0.005	98.9 ± 156	5.1 ± 3.7	1.04 ± 0.71	28.3 ± 30.3	3.8 ± 1.5	2.39 ± 2.36
SN-3	9.0 ± 0.38	1649 ± 1446	10.0 ± 7.0	0.013 ± 0.005	1567 ± 1573	166 ± 173	2.01 ± 4.54	1369 ± 2244	9.6 ± 4.	3.68 ± 4.37
SN-4	8.5 ± 0.24	2396 ± 656	5.7 ± 4.1	0.005 ± 0.001	574.5 ± 307	62.6 ± 47.7	6.38 ± 14.6	5536 ± 2505	10.8 ± 6.2	7.26 ± 5.96
SN-5	8.8 ± 0.53	507 ± 1070	3.3 ± 0.9	0.005 ± 0.003	349 ± 651	105 ± 281	2.08 ± 1.92	713 ± 2328	3.3 ± 1.5	0.58 ± 1.33
SN-6	7.9 ± 0.31	3622 ± 2032	2.7 ± 1.5	0.003 ± 0.001	1053 ± 1644	345 ± 421	0.30 ± 0.62	9533 ± 3758	16.3 ± 8.6	29.0 ± 25.8
SN-7	8.1 ± 0.42	4766 ± 3028	2.1 ± 0.8	0.003 ± 0.001	1225 ± 1685	1495 ± 1951	0.19 ± 0.52	17061 ± 19255	23.2 ± 10.7	4.80 ± 11.1
sWE-1	9.4 ± 0.58	161.6 ± 160	15.7 ± 2.6	0.005 ± 0.004	686 ± 810	996 ± 1177	0.34 ± 0.46	10345 ± 3689	1.3 ± 0.7	0.02 ± 0.03
sWE-2	9.0 ± 0.38	1649 ± 1447	11.0 ± 6.2	0.013 ± 0.005	1567 ± 1573	166.4 ± 173	2.01 ± 4.54	1369 ± 2244	9.6 ± 4.	3.68 ± 4.37
sWE-3	8.6 ± 0.14	468 ± 320	24.5 ± 42.2	0.017 ± 0.004	2208 ± 1865	150 ± 90.4	2.67 ± 2.59	3229 ± 2239	10.8 ± 3.1	0.01 ± 0.01
sWE-4	9.1 ± 0.08	14306 ± 4483	3.4 ± 0.8	0.033 ± 0.020	2941 ± 1214	641 ± 253	2.97 ± 3.73	1443 ± 467	3.0 ± 2.4	0.00 ± 0.00
nWE-A	8.2 ± 0.17	12940 ± 9055	8.5 ± 6.1	0.016 ± 0.012	1375 ± 1247	42.9 ± 18.7	0.70 ± 0.65	1227 ± 832	2.5 ± 1.4	16.9 ± 24.1
nWE-B	8.1 ± 0.42	4647 ± 2917	2.1 ± 0.8	0.003 ± 0.001	1225 ± 1685	1495 ± 1951	0.19 ± 0.52	17061 ± 19255	23.2 ± 10.7	4.80 ± 11.1
nWE-C	8.3 ± 0.10	2283 ± 212	5.1 ± 1.8	0.036 ± 0.032	2471 ± 446	829 ± 273	7.06 ± 4.15	1348 ± 262	4.7 ± 2.7	4.55 ± 5.85
nWE-D	8.7 ± 0.17	8526 ± 9092	9.6 ± 3.1	0.032 ± 0.033	262 ± 89.9	212.6 ± 85.2	0.20 ± 0.30	84.9 ± 97.3	3.9 ± 1.4	1.17 ± 1.87
mWE-I	9.1 ± 0.48	1224 ± 1506	3.54 ± 3.09	0.018 ± 0.011	1567 ± 2205	31.6 ± 34.4	1.48 ± 1.74	415 ± 447	20.7 ± 14.1	0.00 ± 0.00
mWE-II	7.7 ± 0.37	63.9 ± 58.7	3.92 ± 1.11	0.001 ± 0.001	22.3 ± 21.8	10.0 ± 9.4	0.94 ± 0.40	55.6 ± 69.7	5.1 ± 0.6	0.00 ± 0.00
mWE-III	7.9 ± 0.30	3625 ± 2031	2.73 ± 1.45	0.003 ± 0.001	1052 ± 1643	344 ± 421	0.30 ± 0.62	9533 ± 3758	16.5 ± 8.6	32.8 ± 29.0
mWE-IV	8.3 ± 0.29	2534 ± 982	2.37 ± 0.94	0.014 ± 0.005	367 ± 177	266 ± 441	0.17 ± 0.41	7079 ± 3196	6.7 ± 2.1	2.25 ± 3.00
mWE-V	7.9 ± 0.35	2033 ± 961	2.80 ± 1.42	0.050 ± 0.025	522 ± 437	863 ± 634.	0.20 ± 0.41	4330 ± 4343	9.2 ± 5.5	4.20 ± 5.40

Note. Mean values for all three profiles per site are shown with standard deviation. The high standard deviations arise due to the measurement of different soil depths.
*Figure S5 in Supporting Information S1 shows the course of the solublesalts (%) along the three transects.

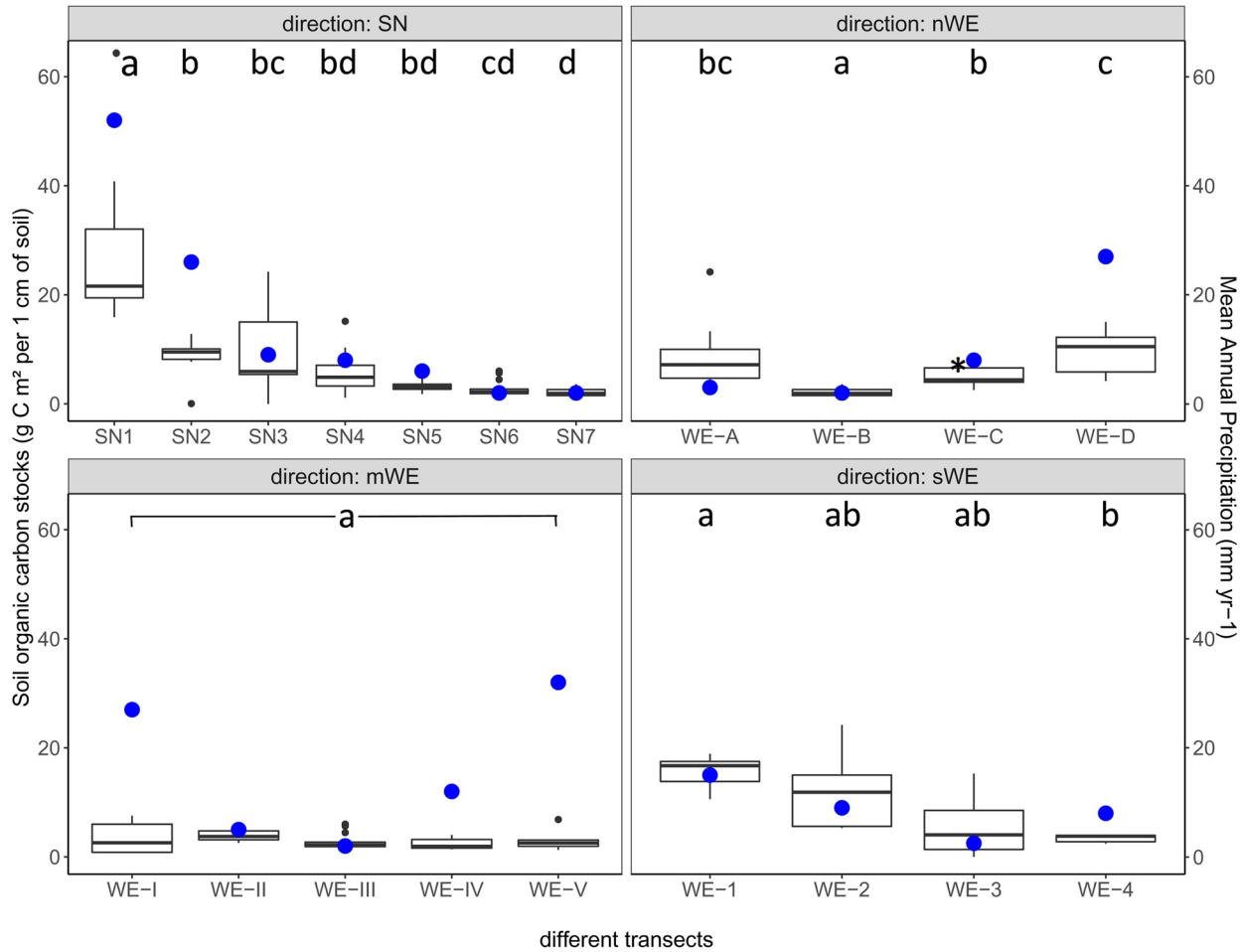

Figure 2. Soil organic carbon stocks (SOC) and precipitation in mm (in blue) along the four different transects. Upper left: South-North gradient shows decreasing SOC stocks. Upper right: northern West-East gradient with increasing SOC stocks with altitude. Lower left: middle West-East gradient with stable SOC stocks. Lower right: southern West-East transect with decreasing SOC stocks with altitude. To sum up: The occurrence of SOC depends in WE direction very much on the latitude. Significance tests for the SOC contents between the directions revealed great differences: SN = b, nWE = ab, mWE = a, sWE = c. **Note*. An outlier with roughly 100 g C m^2 cm^{-1} at plot WE-3 was deleted from the graph for better visibility.

Along the sWE gradient SWC increased clearly with elevation as lowest contents were found at plot sWE-1 near the Pacific coast and highest at plot sWE-4 in the high Andes range. A similar trend was found for mWE transect with the exception of plot mWE-I, where a high SWC was found possibly due to the influence of the coastal fog. Along the altitudinal gradient at the nWE transect SWC was randomly distributed and did not follow any gradients such as aridity or altitude.

3.1.2. Soil Organic Carbon Stocks (Proxy for Habitability)

The SOC stocks along the SN gradient were generally small and decreased significantly tenfold from south to north (Table 3; Table S1 in Supporting Information S1; Figure 2). Along the sWE altitudinal gradient we observed a significant decrease of SOC stocks with altitude ($p < 0.001$) from plot sWE-1 to plot sWE-4, being almost as small as at SN-7. SOC stocks along the mWE transect were comparable at all sites and not significantly different. Along the nWE transect SOC stocks increased with altitude with the exception of nWE-A. Smallest SOC stocks were found again at plot nWE-B (=SN-7), highest at plot nWE-D. We correlated the SOC stocks with MAP and found a strong positive correlation at the SN-transect ($R^2 = 0.8$), positive correlations at the sWE ($R^2 = 0.56$) and the nWE transect ($R^2 = 0.44$) and no correlation at the mWE transect ($R^2 = 0.037$) using Spearman correlation coefficient.

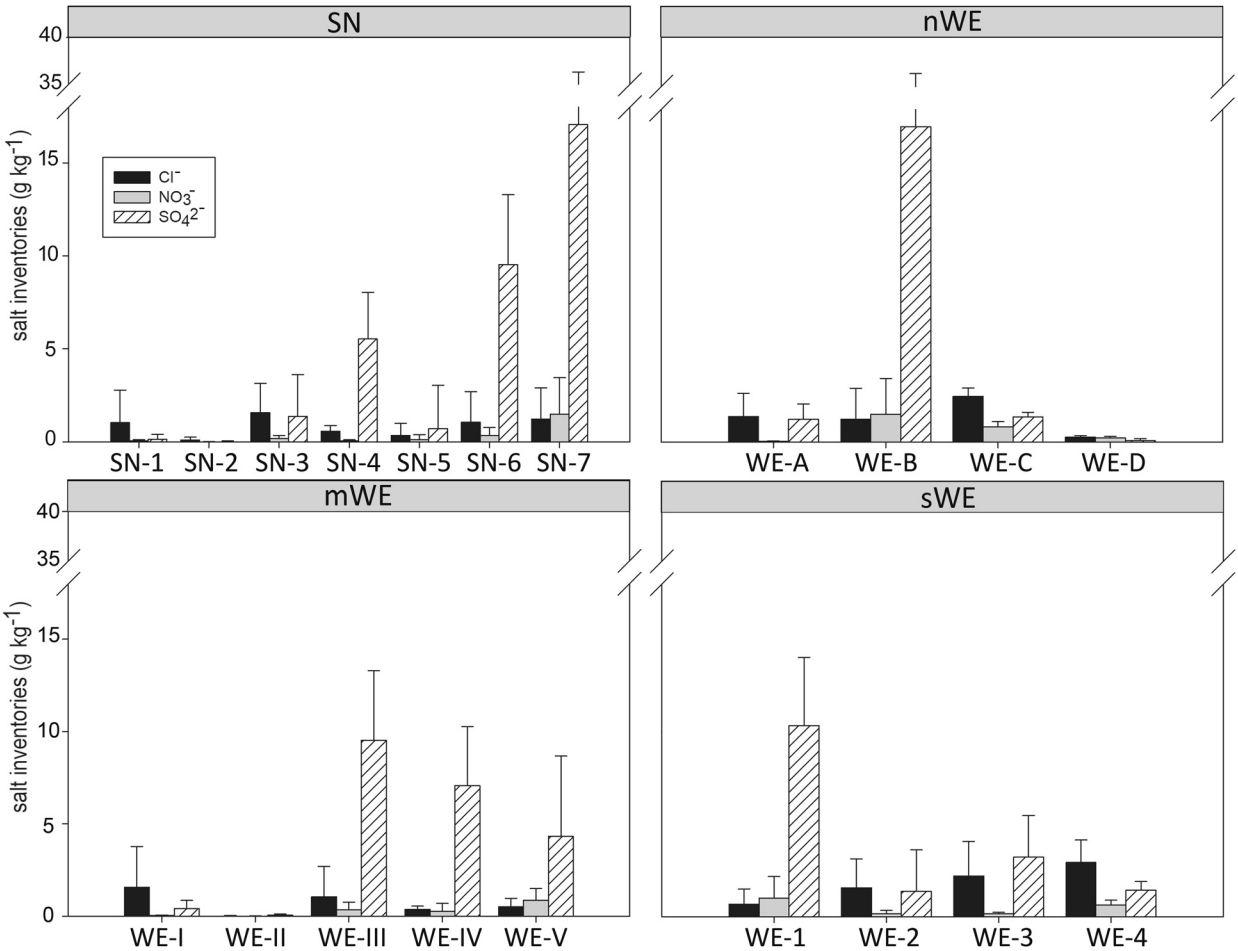

Figure 3. Soil inventory of water-soluble anions up to 60 cm of soil depth determined by ion chromatography along the four investigated transects. Upper left: in South-North direction. Upper right: along the northern West-East transect. Lower left: along the middle West-East transect. Lower right: along the southern West-East transect.

3.1.3. Water-Extractable Ions

Along the South-North aridity gradient the amount of water-extractable ions (Figure 3; Table S1 in Supporting Information S1) increased substantially, mirrored also by the increasing EC (Figure S3 in Supporting Information S1), where small EC comparable to distilled water were found. However at the plots SN-2 and SN-5 total salt concentrations and EC were lower than expected for these latitudes. At the arid plots of SN-1, SN-2 and SN-3 the greatest portion of detected salts were chlorides (50%–82%), followed by sulfates (10%–45%) and to a negligible part also nitrates (3%–5%) occurred. Further to the North in the hyper-arid region (SN-5, SN-6 and SN-7) sulfates dominated with >90% of all detected anions, chlorides took up only 6% and nitrates between 3% and 9%. Phosphates occurred sporadically in soils of all sites with highest contents at the most humid site SN-1.

Along the sWE gradient we found no pattern in the occurrence of water-soluble salts or EC with respect to aridity or altitude (Figures 3 and S4 in Supporting Information S1), although we observed an almost 20fold increase of EC at sWE-4 in the High Andes depending on the soil depth. The content of sulfates was highest at the coast and lowest at plot sWE-2/SN-3. Nitrates were highest at sWE-1 and at the Andean plot sWE-4 but small at sWE-2/SN-3 and sWE-3. Along the mWE transect chlorides showed highest values at the coastal plot mWE-I and the hyper-arid mWE-III/SN-6. Nitrates increased clearly from the coast to the high-altitude sites, while sulfates mainly occurred in the Longitudinal Valley at sites mWE-III and mWE-IV. As a result, EC ranged between 20

µS cm^{-1} at mWE-II and roughly 4000 µS cm^{-1} at plots in the hyper-arid region with single samples >4000 µS cm^{-1} in soil depths below 50 cm. Along the nWE altitudinal gradient sulfates and nitrates showed no clear pattern of occurrence. Largest amounts of sulfates and nitrates were found at nWE-B/SN-7 in the Longitudinal Valley, while nitrates were largely absent at the coast and sulfates at the Andean plot. The concentration of both ions were in stark contrast to the concentrations found at the sWE and the mWE transects, where largest nitrate contents occurred at the coast and high sulfate content at the Andes.

Along the nWE gradient, EC was much larger compared to the other WE gradients. EC ranged between 470 µS cm^{-1} at nWE-D and $3.2{\cdot}10^{4}$ µS cm^{-1} at nWE-A. In contrast to the mWE gradient, EC here followed a trend with decreasing EC from the ocean to the Andes.

3.1.4. Clay Content and pH

The content of clay (Table 3; Figure S3 in Supporting Information S1) varied between all sites, and did not show a pattern along any of the transects. A correlation of clay with SOC or any other soil variable was not observed (Figure S1 in Supporting Information S1).

Along the SN transect, pH decreased in tendency from South to North (Table 3), with SN-1 as an exception having similar pH as at the hyper-arid plots. Along the nWE transect pH tended to increase with altitude. Plot mWE-I at the mWE transect had a mean pH of 9.2 which was significantly higher compared to the other plots at this latitude. In general, pH ranged between 6.9 and 9.9 and a correlation of pH with altitude was not observable.

3.2. Predictors of SOC in the Multivariate Model

The following parameters were included in the model: MAP, SWC, pH, EC, NO_3^-, PO_4^{3-}, SO_4^{2-}, soluble salts, which constitute the portion of lost salts at the washing steps during texture determination as well as kmdistancefromPacific, which is the distance from the Pacific to the sampling site. Seven single explanatory variables had a significant impact on SOC when adding all sampling sites: MAP as the most significant ($p = 1.76{\cdot}10^{-7}$), EC, SWC, NO_3^-, PO_4^{3-}, SO_4^{2-}, CLAY and solublesalts (all with $p \leq 0.01$; data not shown). The rest for example, kmdistancefromPacific and pH were found to be non-significant. Because of the large number of significant explanatory variables, we separated the entire dataset into South-North and West-East direction in order to predict the most affecting parameter along the two different directions separately. Along the South-North directed gradient, only MAP ($p = 6.9{\cdot}10^{-13}$) appeared to be significant (Table 4). In WE direction significant variables were EC, PO_4^{3-}, SO_4^{2-}, CLAY, and MAP (all $p < 0.01$). When running the model with two variables, no other variables became significant beyond of MAP (always $p < 0.001$ in combination) at the SN gradient. In contrast, in West-East direction (Table 5) several combinations appeared to be significant, for example, PO_4^{3-}, SO_4^{2-} and NO_3^- in combination with MAP, kmdistancefromPacific with MAP, or CLAY with kmdistancefromPacific (all $p < 0.01$).

A PCA-biplot showed a clear shift at the SN transect from the arid plots towards the hyper-arid plots (Figure 4a), indicating a gradual change of properties along the gradient and significant differences among the climatic regimes. Salts were positively correlated with each other with the exception of phosphates. SOC, SWC, and MAP were also positively correlated. The loadings indicated by the longest arrows in the biplot showed that MAP, SO_4^{2-}, and SOC had the strongest impact on the separation of the plots. However, salts were uncorrelated to SOC, SWC, and MAP. The PCA also revealed that the plots in the arid region SN-1 and SN-2 were not significantly different from each other, while differing significantly from the hyper-arid cluster comprising SN-6 and SN-7 plots. The PCA for the WE gradients showed that altitude *asl* and *distancefromthePacific* had the strongest impact on the data (Figure 4b), as already suggested by the linear mixed model. These parameters were also positively correlated with each other, with SWC and slightly with MAP. However, SOC was uncorrelated to all of these parameters, which was in contrast to the SN transect where MAP positively correlated with SOC. This means that although a gradient of aridity exists in WE direction, that is, largest humidity at the coast and the Andes, too, a correlation of the occurrence of SOC representing life was not apparent.

Table 4
Mixed Linear Model Regression Result for the South-North Gradient With the Only Significant Individual Parameter "MAP"

Model:	MixedLM	Dependent variable:	SOC			
No. observations:	96	Method:	REML			
No. groups:	7	Scale:	0.5828			
Min. group size:	11	Log-Likelihood:	−116.9414			
Max. group size:	15	Converged:	Yes			
Mean group size:	13.7					
	Coef.	Std.Err.	z	$p > \|z\|$	[0.025	0.975]
Intercept	0.949	0.142	6.666	0.000	0.670	1.228
MAP	0.044	0.006	7.181	0.00***	0.032	0.056
Group Var	0.036	0.071				

Note. Along SN direction, the model is stable also when two or all parameters are included (data not shown), always leading to the same result: only *MAP* is significant on the occurrence of SOC pointing toward a genuine SN-aridity gradient. Asterisks indicate significance levels: * if $p < 0.05$, ** if $p < 0.01$, and *** if $p < 0.001$. p values for the non-significant variables were: EC ($p = 0.871$), pH ($p = 0.658$), SWC ($p = 0.3$), Cl^- ($p = 0.836$), NO_3^- ($p = 0.627$), PO_4^{3-} ($p = 0.54$), SO_4^{2-} ($p = 0.607$), CLAY ($p = 0.069$), soluble salts ($p = 0.134$), kmdistancefromPacific ($p = 0.342$).

4. Discussion

4.1. Parameters Affected by Aridity

Much research has been published in the past on how environmental parameters like aridity affect the occurrence of life in the Atacama Desert, often with respect to conditions on Mars. We found in our comparative study along four separate transects that the occurrence of SOC, which we use as an indicator for habitability, decreased as expected in SN-direction because of decreasing water availability, while its occurrence in WE-direction depended on the latitudinal location of the transect and several other geographic and physico-chemical properties.

SOC content declined with increasing aridity along the SN-gradient (Figure 2) which is in agreement with field observations of the loss of above-ground vegetation and with other studies sampling in South-North direction

Table 5
Mixed Linear Model Regression Result for the West-East Gradients With Two Parameters Included

Model:	MixedLM	Dependent variable:	SOC			
No. observations:	136	Method:	REML			
No. groups:	3	Scale:	0.2212			
Min. group size:	36	Log-Likelihood:	−95.5314			
Max. group size:	0.53	Converged:	Yes			
Mean group size:	42.3					
	Coef.	Std.Err.	z	$p > \|z\|$	[0.025	0.975]
Intercept	1.516	0.352	4.311	0.000	0.827	2.205
MAP	0.036	0.008	4.603	0.00***	0.021	0.051
kmdistancefromPacif.	−0.003	0.001	−3.958	0.00***	−0.005	−0.002
Group Var	0.341	0.494				

Note. Several other duo-combinations were significant as well, for example, MAP ($p = 0.008$) & EC ($p = 0.008$), MAP ($p = 0.032$) & pH ($p = 0.541$), MAP ($p = 0.001$) & NO_3^- ($p = 0.008$) etc., pointing toward several different parameters affecting the occurrence of SOC. By this, the WE direction constitutes transects rather than real gradients. Asterisks indicate significance levels: * if $p < 0.05$, ** if $p < 0.01$, and *** if $p < 0.001$. When running the SN gradient with only two parameters, only MAP appeared to be significant at all duo combinations, for example, MAP ($p < 0.001$) & EC ($p = 0.943$), MAP ($p < 0.001$) & pH ($p = 0.823$), MAP ($p < 0.001$) & Cl^- ($p = 0.976$), MAP ($p < 0.001$) & SWC ($p = 0.82$), MAP ($p < 0.001$) & CLAY ($p = 0.201$), etc.

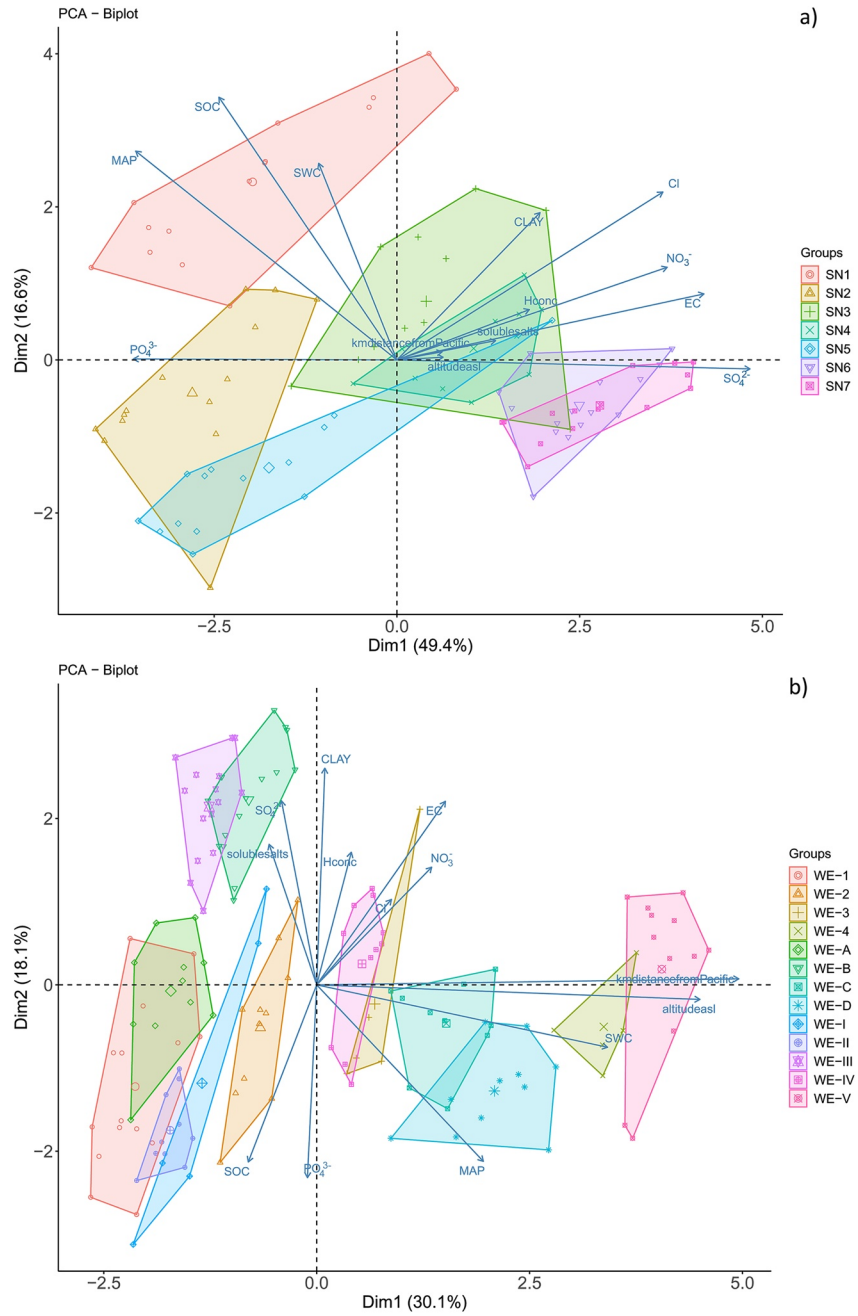

Figure 4. (a) Principal Component Analysis (PCA) for the South-North gradient. Salts, pH, and CLAY (with the exception of PO_4^{3-}) correlate positively with each other, while SOC, SWC, and MAP is correlated positively with each other. The length of the variable's arrows indicate the grade of impact on the sites. A clear shift from the arid plots SN-1 and SN-2 toward the hyper-arid plots SN-6 and SN-7 indicates a gradual change of properties along the gradient and significant differences among the climatic regimes. (b) The PCA along the three West-East transects shows that altitude asl and distance from the Pacific have the strongest impact on the data. They are positively correlated with each other, with SWC and with MAP but uncorrelated with SOC which is in contrast to the SN gradient, where the occurrence of SOC is positively correlated with precipitation.

(Crits-Christoph et al., 2013). SOC contents coincide to the findings of other studies (Connon et al., 2007; Crits-Christoph et al., 2013; Ewing et al., 2008; Pfeiffer et al., 2020) and lie well below concentrations of other deserts, like the Northern Negev desert (minimum of 2.3 g kg^{-1} in autumn in the driest season; Amundson, 2001; Barness et al., 2009). We suggest the decline to be a direct result of the decrease of water availability as water

drives primary production (Lawlor, 2002). In the hyper-arid region (SN-5, SN-6, and SN-7), SOC contents are very small pointing towards a very limited primary production at the surface and small abundance of heterotrophic communities in deeper soil depths which was suggested for the entire hyper-arid core (Warren-Rhodes et al., 2006). At the sWE and the nWE transect, SOC contents increased with altitude and correlated slightly with MAP, although the correlation was less pronounced compared to the SN gradient. In contrast, at the mWE transect SOC contents were uncorrelated with MAP as at this latitude high MAP occurred at the coast and in the Andes, while SOC contents were stable, suggesting the existence of another abiotic variable that limits SOC. An explanation might be the increased radiation with altitude or lower temperature. Harmful UV-A and UV-B increases by 4% respectively 9% per km of altitude between 0 and 2500 m a.s.l. and 4% respectively 2% per km between 2500 and 5100 m a.s.l (Cordero et al., 2018). As radiation inhibits primary production and also leads to enhanced photodegradation of organic molecules, a shortcut in which CO_2 is produced from decaying plants and released into the atmosphere, altitude may well explain the decreasing SOC stocks along the sWE (max. altitude of 4343 m asl) and mWE (max. altitude of 3973 m asl) transects. Our nWE gradient ended at a maximum altitude of 2535 m asl (plot nWE-D), thus biologic activity may not have been impacted by increased radiation yet. However, nWE-D lies even higher than mWE-IV, but has considerably larger SOC contents proving altitude not to be the influencing parameter on SOC at nWE-D. Diaz et al. (2016) found along a threefold-dimensional gradient ranging from 2700 to 4500 m a.s.l. with increasing mean annual precipitation (MAP) and decreasing mean annual temperature (MAT) a strong correlation (R^2~0.9) between those three variables. Although their result suggests a dependency of SOC by MAP and MAT, MAP and MAT are highly confounding, which again highlights the need to reduce the number of environmental variables to avoid multidimensional data.

The increasing aridity along the SN aridity gradient is mirrored also by the more abundant water-soluble salts such as sulphates and nitrates the drier the climate becomes. Lybrand et al. (2016) observed nitrate concentrations ranging between 45.4 g kg^{-1} and 324 g kg^{-1} at nitrate deposits in the hyper-arid region north of SN-7, which correspond to our findings (roughly 30–90 g kg^{-1}). These salts are transported to the Central Valley from various sources like the Salares (salt lakes), the Pacific Ocean or from volcanic emissions via dry or wet deposition, where they precipitate during evaporation and accumulate (Carmona et al., 2000; Ewing et al., 2006; Houston, 2006; Rech et al., 2003). The large abundance of chlorides at plots SN-1 and SN-3 was surprising as chlorides are easily-soluble salts, thus, they were expected to rather abound at hyper-arid than at the comparably wetter sites. Small amounts of salts were detected at the hyper-arid plot SN-5. Small SWC and the absence of vegetation/lichens exclude the possibility that SN-5 receives more frequent precipitation leading to the leaching of salts to deeper depths beyond sampling. However, its sandy soil texture possibly allows faster leaching of ions as sand retains only little moisture. However, the immense difference in the salt content between SN-5 and the other two hyper-arid plots may possibly not be explained by texture alone. Instead, the small salt contents point towards a decoupling of salts from aridity meaning that the deposition and accumulation of salts are dictated by local factors (Ewing et al., 2006) and not only by aridity. Along the nWE gradient only nitrate shows a distinct pattern as its concentration decrease with increasing distance from the Salares where they originate from (Rech et al., 2003). Along the sWE altitudinal gradient salt inventories of the different species also do not show a distinct pattern, and remain quite stable with the exception of plot sWE-1 at the coast. Thus, we could not show a correlation of salts with altitude or aridity. Taken together, the results reveal that a higher sampling resolution in the hyper-arid core along the climatic gradient is needed as processes differ considerably between sites which receive similar amounts of precipitation. The huge heterogeneity of the soils in the Atacama within hyper-arid climatic conditions may also have implications for the search of life on Mars, where the occurrence of nitrates and gypsum is even more widespread than in the Atacama Desert (Flahaut et al., 2010; Gendrin et al., 2005). Voigt et al. (2020) found a correlation of salt inventories with aridity along their latitudinal gradient. Thus, salts are a potentially useful indicators for aridity, but their sheer existence does not necessarily reflect hyper-arid conditions and their absence does not necessarily indicate wetter conditions, as they depend also on the input situation and the release by weathering.

4.2. Parameters Affected by Multiple Driving Factors

Given the potential misconception about the nature and direction of Atacama gradients, the existing body of studies display a mixed level of quality (Table 1). The greatest part of the cited working groups laid great effort on a proper sampling scheme for their research question. However, some of the studies used the single sampling or even arbitrary site selection in their experimental set-up, whereas gradients would have been more appropriate

and would have likely resulted in improved process understanding. Other authors used altitudinal gradients, thus their results always mirror a mixture of the different climatic regimes of the coast, the dry desert and the Andes. For example, Mandakovic et al. (2018) sampled across an aridity, pH, and altitudinal gradient west of the Salar de Atacama and showed that the soil properties differed significantly between the sites depending on altitude. Thus, besides the erratic availability of water, altitudinal effects like enhanced UV radiation and lower temperature are confounded as all influence the results, making conclusions ambiguous.

4.3. Factoral Stabilities and Arbitrary Mixtures Along Gradient Directions

Due to multiple impacting factors on the occurrence of SOC, like fog, altitude, aridity, salt inventories, which exist in the Atacama, the application of deeper multivariate statistics might be useful when working on large-scale gradient studies. Rillig et al. (2019) investigated the effects of explanatory variables in multivariate gradients using Random Forest classification and showed that deleting variables one by one from the dataset will result in a significantly altered output. Conversely, this means that defining only one changing parameter along the desired gradient is crucial to avoid later misinterpretation of results. For example, along aridity gradients, which are used for Martian analogue studies, aridity should be the only parameter that changes, while other geographic variables like altitude or distance from the ocean should remain constant. We found that in South-North direction, the only significant variable is MAP, as expected for a genuine aridity gradient. This suggests, that the proposed direction might be a well-chosen aridity gradient with the availability of water being the most dominant property. This is supported also by the gradually decreasing SWC toward the north, with similar values reported by Horikoshi (2011).

In contrast, at the WE direction several properties affect habitability as indicated by SOC, complicating the correct assignment of significant predictors on the parameter of interest. Here, precipitation and the availability of water (SWC) does not seem to play a large role, instead the distance from the Pacific and with it the altitude asl were the dominating parameters. This result was surprising as the precipitation corresponds well with the SOC contents at least at two of the transects (nWE and sWE), and also the SWC along the mWE- and sWE-transects increased with altitude. The Northern Chilean landscapes with its complex geography might explain some of these results. Due to the inverse climatic conditions and the diverging altitude of the Coastal Cordillera, which stretches along the Pacific coast from South to North, a humidity-rich fog forms at the coast and can reach into the desert up to 40 km but in differing amounts depending on the altitude of the Coastal Cordillera. That means, that sites along the coast and also up to 40 km away from the coast receive different amounts of water depending on their longitudinal position, thus, depending on the possibility of the fog to reach inland. For example, site mWE-I located at a latitude with hyper-arid conditions in the Central Valley is vegetated year-round by Cactaceae as the fog cannot overcome the sudden and extreme rise of the mountain chain and remains here. Further to the South, thus further away from hyper-aridity, the coastal plot sWE-1 remains much drier as the Coastal Cordillera reaches maximum 1200 m a.s.l. allowing the Camanchaca fog to pass this site and to penetrate inland (Rech et al., 2003). Thus, fog enables life at the coast at latitudes where without the Coastal Cordillera life-limiting, hyper-arid conditions would prevail. Beyond 100 km from the coast and above 2300 m a.s.l., frontal winter precipitation occurs that increases exponentially with altitude (Houston, 2006). Thus, the WE-plots at high altitudes are influenced by temporal (e.g., snowmelt in austral spring) and spatial patterns of precipitation delivered from the Eastern side of the Andes that does not reach the Central Valley. While we sampled during austral summer, the increased SWC at higher altitudes suggest that the SWC was either the remnant of the winter precipitation, of snow melt or of recent precipitation events, however, did not significantly affect the occurrence of SOC. This highlights that precipitation and, as a consequence, SWC along altitudinal transects are driven by the likeliness to be influenced by Camanchaca at the coast and the scavenging of rain by the Andes. This contrasts the SN aridity gradient where stable climatic conditions allow for reliable predictions of habitability in terms of water availability throughout the year.

Although we put great effort to establish three WE oriented soil transects as analogue transects, we propose not to use this orientation for Martian analogue studies as this sampling direction turned out to be a multi-parameter gradient strongly confounded by the heterogeneous landscapes of the Atacama Desert making predictions and evaluations on habitability complicated if not impossible. Thus, with respect to Martian analogue studies along aridity, the results indicate that in the Atacama the established climatic gradient from South to North is more convincing as this turned out to be a one-parameter gradient, that is, only aridity is changing. Additionally, it comprises a larger spatial width in the different climatic areas enabling several sampling sites at

hyper-arid conditions compared to W-E sampling where conditions change at a fast pace. Nevertheless, it must be clearly stated that promising analogue site identification in SN direction is rather limited to the central depression between the Coastal Cordillera and the Central Cordillera. A shift of SN gradients towards the coast would result in an arbitrary mixture of topography-driven coastal fog amendments as would a shift towards the Andes result in altitudinal driven precipitation scavenging, as is easily deducible by a comparison of the SN transects constituted by the southern, middle and northern part of the WE transects (Figure 2). This explains why analogue sites like Yungay are largely and justifiably accepted by the research community. Discovering processes out of one sampling site per climatic regime remains challenging. Notably, the South-North gradient revealed also differences between the sites suggesting local processes, for example, the de-coupling of salts and the state of aridity. Differences between sites exist and the use of a proper gradient helps to detect such processes. When looking for analogue sites, this heterogeneity has to be accepted and even actively searched for.

5. Conclusions

Here we evaluated process interactions in the Atacama Desert along contrasting gradients parallel and perpendicular to the Ocean and the Andes to reveal the best possible sampling direction for analogue and habitability research. In the Atacama Desert, this is best achieved by using a climatic gradient in South-North direction in the Central Valley. The SN gradient resulted to be an apt testing ground for natural experiments as it has a gradually increasing aridity while other influencing parameters on SOC were excluded. The decreasing precipitation lead to a gradual decline of the soil water content, the SOC stocks and an increase of salt contents. In contrast, the West-East gradients resulted in an erratic influence of multiple parameters such as altitude, distance from the Pacific, and MAP, making the evaluation of the most influencing parameter on the occurrence of SOC, which we regard as an appromixation to life**,** difficult. We could show that many drivers of habitability in deserts are only mistakenly attributed to aridity alone, thus obscuring a clear view of the far more complex process interactions. Additionally it was found that the often applied aridity index defined by the UNEP does not reflect the true aridity status of sites in the Atacama Desert, as it does not respect coastal fog development or air humidity scavenging by salt concretions in soil, nor does it sufficiently provide resolution for the investigated area. Our findings further highlight the necessity to reduce the number of environmental variables in process-oriented gradient research in order to enhance predictability of the parameter of interest. Honest analogue research has to examine and clearly allot the contribution of marine or terrestrial sources of for example, SWC and SOC outside of the analogue site itself, as these impose clear differences to the contemporary situation on Mars, potentially leading to questionable conclusions.

Conflict of Interest

The authors declare no competing financial conflicts of interest with this study.

Data Availability Statement

All measured data, reported in this study, are available at https://zenodo.org/record/5665146.

Acknowledgments
The authors wish to thank the German Research Foundation (DFG) for funding of this study in the frame of the German-Chilean joint priority research project SPP 1803 *EarthShape* (BO3741/4-1). We received invaluable support in the laboratory from Ulrike Pieper, Anne Herwig, Jan-Philip Dieck, Talitha Henneking and several other wonderful collegues for whose help we are very grateful. R.M. was supported by the DLR grant FuE-Projekt "ISS LIFE" (Programm RF-FuW, Teilprogramm 475). We thank the anonymous reviewers for their very helpful advice. Open access funding enabled and organized by Projekt DEAL.

References

Alboukadel, K., & Mundt, F. (2020). *factoextra: Extract and visualize the results of multivariate data analysis. R package version 1.0.7*. Retrieved from https://CRAN.R-project.org/package=factoextra

Amundson, R. (2001). The carbon budget in soils. *Annual Review of Earth and Planetary Sciences*, *29*(1), 535–562. https://doi.org/10.1146/annurev.earth.29.1.535

Araújo, M. B., & Guisan, A. (2006). Five (or so) challenges for species distribution modelling. *Journal of Biogeography*, *33*(10), 1677–1688. https://doi.org/10.1111/j.1365-2699.2006.01584.x

Arriagada, J. (2016). Elaboración de una base digital del clima comunal de Chile: Línea base (1980–2010) y proyección al año 2050. Estudio encargado por el Ministerio del Medio Ambiente Departamento de Cambio Climático. Informe final. With the help of K.-P. Muck. Ministerio del Medio Ambiente Departamento de Cambio Climático. Retrieved from https://mma.gob.cl/cambio-climatico/

Aszalós, J. M., Szabó, A., Megyes, M., Anda, D., Nagy, B., & Borsodi, A. K. (2016). Bacterial diversity of a high-altitude permafrost thaw pond located on Ojos del Salado (Dry Andes, Altiplano-Atacama region). *Astrobiology*, *20*(6), 754–765. https://doi.org/10.1089/ast.2018.2012

Austin, M. P., & Niel, K. P. (2011). Improving species distribution models for climate change studies. Variable selection and scale. *Journal of Biogeography*, *38*(1), 1–8. https://doi.org/10.1111/j.1365-2699.2010.02416.x

Azua-Bustos, A., Fairén, A. G., González-Silva, C., Ascaso, C., Carrizo, D., Fernández-Martínez, M. Á., et al. (2018). Unprecedented rains decimate surface microbial communities in the hyperarid core of the Atacama Desert. *Scientific Reports*, *8*(1), 16706. https://doi.org/10.1038/s41598-018-35051-w

Azua-Bustos, A., González-Silva, C., Fernández-Martínez, M. A., Arenas-Fajardo, C., Fonseca, R., Martín-Torres, F. J., et al. (2019). Aeolian transport of viable microbial life across the Atacama Desert, Chile. Implications for Mars. *Scientific Reports*, *9*(1), 11024. https://doi.org/10.1038/s41598-019-47394-z

Barness, G., Rodriguez Zaragoza, S., Shmueli, I., & Steinberger, Y. (2009). Vertical distribution of a soil microbial community as affected by plant ecophysiological adaptation in a desert system. *Microbial Ecology*, *57*(1), 36–49. https://doi.org/10.1007/s00248-008-9396-5

Barrow, C. J. (1992). World atlas of desertification (United Nations environment programme), edited by N. Middleton and D. S. G. Thomas. Edward Arnold, London, 1992. ISBN: 0 340 55512 2. Land Degradation & Development, *3*(4), 249. https://doi.org/10.1002/ldr.3400030407

Barry, R. G. (1992). Mountain weather and climate. *Routledge Physical Environment Series* (2nd ed.). London: Routledge.

Billi, D., Verseux, C., Fagliarone, C., Napoli, A., Baqué, M., & Vera, J.-P. (2019). A desert cyanobacterium under simulated Mars-like conditions in low earth orbit. Implications for the habitability of Mars. *Astrobiology*, *19*(2), 158–169. https://doi.org/10.1089/ast.2017.1807

Brantley, S. L., Megonigal, J. P., Scatena, F. N., Balogh-Brunstad, Z., Barnes, R. T., Bruns, M. A., et al. (2011). Twelve testable hypotheses on the geobiology of weathering. *Geobiology*, *9*(2), 140–165. https://doi.org/10.1111/j.1472-4669.2010.00264.x

Bretz, F., Hothorn, T., & Westfall, P. H. (2011). *Multiple comparisons using R*. Boca Raton, FL: Chapman & Hall/CRC Press.

Burgener, L., Huntington, K. W., Hoke, G. D., Schauer, A., Ringham, M. C., Latorre, C., & Díaz, F. P. (2016). Variations in soil carbonate formation and seasonal bias over >4 km of relief in the western Andes (30°S) revealed by clumped isotope thermometry. *Earth and Planetary Science Letters*, *441*(1–4), 188–199. https://doi.org/10.1016/j.epsl.2016.02.033

Carmona, V., Pueyo, J. J., Taberner, C., Chong, G., & Thirlwall, M. (2000). Solute inputs in the salar de Atacama (N Chile). *Journal of Geochemical Exploration*, *69–70*, 449–452. https://doi.org/10.1016/s0375-6742(00)00128-x

Casanova, M., Salazar, O., Seguel, O., & Luzio, W. (2013). The soils of Chile. *World Soils Book Series*. Springer. https://doi.org/10.1007/978-94-007-5949-7

Clarke, J. D. A. (2006). Antiquity of aridity in the Chilean Atacama Desert. *Geomorphology*, *73*(1–2), 101–114. https://doi.org/10.1016/j.geomorph.2005.06.008

Connon, S. A., Lester, E. D., Shafaat, H. S., Obenhuber, D. C., & Ponce, A. (2007). Bacterial diversity in hyperarid Atacama Desert soils. *Journal of Geophysical Research*, *112*(G4). https://doi.org/10.1029/2006jg000311

Contreras, S., Lange, C. B., Pantoja, S., Lavik, G., Rincón-Martínez, D., & Kuypers, M. M. M. (2010). A rainy northern Atacama Desert during the last interglacial. *Geophysical Research Letters*, *37*(23). https://doi.org/10.1029/2010gl045728

Cordero, R. R., Damiani, A., Jorquera, J., Sepúlveda, E., Caballero, M., Fernandez, S., et al. (2018). Ultraviolet radiation in the Atacama Desert. *Antonie van Leeuwenhoek*, *111*(8), 1301–1313. https://doi.org/10.1007/s10482-018-1075-z

Cortesão, M., Fuchs, F. M., Commichau, F. M., Eichenberger, P., Schuerger, A. C., Nicholson, W. L., et al. (2019). Bacillus subtilis spore resistance to simulated Mars surface conditions. *Frontiers in Microbiology*, *10*, 333. https://doi.org/10.3389/fmicb.2019.00333

(CR)2. (2018). *Valores mensuales de precipitación medidos desde estaciones nacionales, desde 1900 al presente año*. CR2_prAmon_2018.zip. Santiago de Chile, Chile: Center for Climate and Resilience Research. Retrieved from https://www.cr2.cl/eng/?s=pramon

Crits-Christoph, A., Robinson, C, K., Barnum, T., Fricke, W. F., Davila, A. F., & Jedynak, B. (2013). Colonization patterns of soil microbial communities in the Atacama Desert. *Microbiome*, *1*(1), 28. https://doi.org/10.1186/2049-2618-1-28

Davila, A. F., Gómez-Silva, B., Rios, A., Ascaso, C., Olivares, H., McKay, C. P., & Wierzchos, J. (2008). Facilitation of endolithic microbial survival in the hyperarid core of the Atacama Desert by mineral deliquescence. *Journal of Geophysical Research*, *113*(G1). https://doi.org/10.1029/2007jg000561

Davila, A. F., Hawes, I., Ascaso, C., & Wierzchos, J. (2013). Salt deliquescence drives photosynthesis in the hyperarid Atacama Desert. *Environmental Microbiology Reports*, *5*(4), 583–587. https://doi.org/10.1111/1758-2229.12050

Davis, W. L., Pater, I., & McKay, C. P. (2010). Rain infiltration and crust formation in the extreme arid zone of the Atacama Desert, Chile. *Planetary and Space Science*, *58*(4), 616–622. https://doi.org/10.1016/j.pss.2009.08.011

Demergasso, C., Casamayor, E. O., Chong, G., Galleguillos, P., Escudero, L., & Pedrós-Alió, C. (2006). Distribution of prokaryotic genetic diversity in athalassohaline lakes of the Atacama Desert, Northern Chile. *FEMS Microbiology Ecology*, *48*(1), 57–69. https://doi.org/10.1016/j.femsec.2003.12.013

DGAC. (2021). *Dirección Meteorológica de Chile*. Av. Portales 3450, Estación Central, Santiago de Chile, Chile. Retrieved from https://climatologia.meteochile.gob.cl/

Diaz, F. P., Frugone, M., Gutiérrez, R. A., & Latorre, C. (2016). Nitrogen cycling in an extreme hyperarid environment inferred from δ(15)N analyses of plants, soils and herbivore diet. *Scientific Reports*, *6*, 22226. https://doi.org/10.1038/srep22226

Dong, H., Rech, J. A., Jiang, H., Sun, H., & Buck, B. J. (2007). Endolithic cyanobacteria in soil gypsum. Occurrences in Atacama (Chile), Mojave (United States), and Al-Jafr basin (Jordan) deserts. *Journal of Geophysical Research*, *112*(G2), 1053. https://doi.org/10.1029/2006jg000385

Drees, K. P., Neilson, J. W., Betancourt, J. L., Quade, J., Henderson, D. A., Pryor, B, M., & Maier, R. M. (2006). Bacterial community structure in the hyperarid core of the Atacama Desert, Chile. *Applied and Environmental Microbiology*, *72*(12), 7902–7908. https://doi.org/10.1128/aem.01305-06

Ewing, S. A., Macalady, J. L., Warren-Rhodes, K., McKay, C. P., & Amundson, R. (2008). Changes in the soil C cycle at the arid-hyperarid transition in the Atacama Desert. *Journal of Geophysical Research*, *113*(G2). https://doi.org/10.1029/2007jg000495

Ewing, S. A., Sutter, B., Owen, J., Nishiizumi, K., Sharp, W., Cliff, S. S., et al. (2006). A threshold in soil formation at Earth's arid-hyperarid transition. *Geochimica et Cosmochimica Acta*, *70*(21), 5293–5322. https://doi.org/10.1016/j.gca.2006.08.020

Finstad, K., Pfeiffer, M., McNicol, G., Barnes, J., Demergasso, C., Chong, G., & Amundson, R. (2016). Rates and geochemical processes of soil and salt crust formation in Salars of the Atacama Desert, Chile. *Geoderma*, *284*, 57–72. https://doi.org/10.1016/j.geoderma.2016.08.020

Finstad, K. M., Probst, A. J., Thomas, B. C., Andersen, G. L., Demergasso, C., & Echeverría, A. (2017). Microbial community structure and the persistence of cyanobacterial populations in salt crusts of the hyperarid Atacama Desert from genome-resolved metagenomics. *Frontiers in Microbiology*, *8*, 1435. https://doi.org/10.3389/fmicb.2017.01435

Flahaut, J., Quantin, C., Allemand, P., Thomas, P., & Le Deit, L. (2010). Identification, distribution and possible origins of sulfates in Capri Chasma (Mars), inferred from CRISM data. *Journal of Geophysical Research*, *115*(E11), 499. https://doi.org/10.1029/2009je003566

Fletcher, L. E., Valdivia-Silva, J. E., Perez-Montaño, S., Condori-Apaza, R. M., Conley, C. A., & McKay, C. P. (2012). Variability of organic material in surface horizons of the hyper-arid Mars-like soils of the Atacama Desert. *Advances in Space Research*, *49*(2), 271–279. https://doi.org/10.1016/j.asr.2011.10.001

Galloway, J. N., Dentener, F. J., Capone, D. G., Boyer, E. W., Howarth, R. W., Seitzinger, S. P., et al. (2004). Nitrogen cycles. Past, present, and future. *Biogeochemistry*, *70*(2), 153–226. https://doi.org/10.1007/s10533-004-0370-0

Galun, M. (2019). Handbook of lichenology. *Routledge Revivals Series* (Vol. 3). Milton: CRC Press LLC.
García-Descalzo, L., Parro, V., García-Villadangos, M., Cockell, C. S., Moissl-Eichinger, C., Perras, A., et al. (2019). Microbial markers profile in anaerobic Mars analogue environments using the LDChip (life detector chip) antibody microarray core of the SOLID (signs of life detector) platform. *Microorganisms*, *7*(9). https://doi.org/10.3390/microorganisms7090365
Gendrin, A., Mangold, N., Bibring, J.-P., Langevin, Y., Gondet, B., Poulet, F., et al. (2005). Sulfates in Martian layered terrains. The OMEGA/Mars Express view. *Science (New York, N.Y.)*, *307*(5715), 1587–1591. https://doi.org/10.1126/science.1109087
Gillison, A. N., & Brewer, K. R. W. (1985). The use of gradient directed transects or gradsects in natural-resource surveys. *Journal of Environmental Management*, *20*(2), 103–127.
Gómez-Silva, B. (2018). Lithobiontic life. "Atacama rocks are well and alive". *Antonie van Leeuwenhoek*, *111*(8), 1333–1343. https://doi.org/10.1007/s10482-018-1033-9
Harris, D., Horwáth, W. R., & Kessel, C. (2001). Acid fumigation of soils to remove carbonates prior to total organic carbon or CARBON-13 isotopic analysis. *Soil Science Society of America Journal*, *65*(6), 1853–1856. https://doi.org/10.2136/sssaj2001.1853
Hartley, A. J., Chong, G., Houston, J., & Mather, A. E. (2005). 150 million years of climatic stability. Evidence from the Atacama Desert, northern Chile. *Journal of the Geological Society*, *162*(3), 421–424. https://doi.org/10.1144/0016-764904-071
Hayashi, M. (2004). Temperature-electrical conductivity relation of water for environmental monitoring and geophysical data inversion. *Environmental Monitoring and Assessment*, *96*, 119–128. https://doi.org/10.1023/b:emas.0000031719.83065.68
Horikoshi, K. (Ed.). (2011). *Extremophiles handbook*. Tokyo: Springer (Springer reference).
Houston, J. (2006). Variability of precipitation in the Atacama Desert. Its causes and hydrological impact. *International Journal of Climatology*, *26*(15), 2181–2198. https://doi.org/10.1002/joc.1359
Houston, J., & Hartley, A. J. (2003). The central Andean west-slope rainshadow and its potential contribution to the origin of hyper-aridity in the Atacama Desert. *International Journal of Climatology*, *23*(12), 1453–1464. https://doi.org/10.1002/joc.938
IUSS Working Group WRB. (2015). World reference base for soil resources 2014. Update 2015. International soil classification system for naming soils and creating legends for soil maps. Rome (World soil resources reports no. 106).
Kite, E. S., Mayer, D. P., Wilson, S. A., Davis, J. M., Lucas, A. S., & Stucky de Quay, G. (2019). Persistence of intense, climate-driven runoff late in Mars history. *Science Advances*, *5*(3), eaav7710. https://doi.org/10.1126/sciadv.aav7710
Knief, C., Bol, R., Amelung, W., Kusch, S., Frindte, K., Eckmeier, E., et al. (2020). Tracing elevational changes in microbial life and organic carbon sources in soils of the Atacama Desert. *Global and Planetary Change*, *184*, 103078. https://doi.org/10.1016/j.gloplacha.2019.103078
Lawlor, D. W. (2002). Limitation to photosynthesis in water-stressed leaves. Stomata vs. metabolism and the role of ATP. *Annals of Botany*, *89*, 871–885. https://doi.org/10.1093/aob/mcf110
Liu, D., Peñuelas, J., Ogaya, R., Estiarte, M., Tielbörger, K., Slowik, F., et al. (2018). Species selection under long-term experimental warming and drought explained by climatic distributions. *New Phytologist*, *217*(4), 1494–1506. https://doi.org/10.1111/nph.14925
Lybrand, R. A., Bockheim, J. G., Ge, W., Graham, R. C., Hlohowskyj, S. R., Michalski, G., et al. (2016). Nitrate, perchlorate, and iodate co-occur in coastal and inland deserts on Earth. *Chemical Geology*, *442*, 174–186. https://doi.org/10.1016/j.chemgeo.2016.05.023
Mandakovic, D., Rojas, C., Maldonado, J., Latorre, M., Travisany, D., Delage, E., et al. (2018). Structure and co-occurrence patterns in microbial communities under acute environmental stress reveal ecological factors fostering resilience. *Scientific Reports*, *8*(1), 5875. https://doi.org/10.1038/s41598-018-23931-0
Mayer, M. (2019). *missRanger: Fast imputation of missing values*. Retrieved from https://CRAN.R-project.org/package=missRanger
McKay, C. P., Friedmann, E. I., Gómez-Silva, B., Cáceres-Villanueva, L., Andersen, D. T., & Landheim, R. (2004). Temperature and moisture conditions for life in the extreme arid region of the Atacama Desert: Four years of observations including the El Niño of 1997–1998. *Astrobiology*, *3*(2), 393–406. https://doi.org/10.1089/153110703769016460
Meslier, V., Casero, M. C., Dailey, M., Wierzchos, J., Ascaso, C., Artieda, O., et al. (2018). Fundamental drivers for endolithic microbial community assemblies in the hyperarid Atacama Desert. *Environmental Microbiology*, *20*(5), 1765–1781. https://doi.org/10.1111/1462-2920.14106
Metz, J., Tielbörger, K., & Michalet, R. (2015). Spatial and temporal aridity gradients provide poor proxies for plant-plant interactions under climate change. A large-scale experiment. *Functional Ecology*, *30*(1), 20–29. https://doi.org/10.1111/1365-2435.12599
Michalski, G., Böhlke, J. K., & Thiemens, M. (2004). Long term atmospheric deposition as the source of nitrate and other salts in the Atacama Desert, Chile. New evidence from mass-independent oxygen isotopic compositions. *Geochimica et Cosmochimica Acta*, *68*(20), 4023–4038. https://doi.org/10.1016/j.gca.2004.04.009
Nagy, B., Ignéczi, Á., Kovács, J., Szalai, Z., & Mari, L. (2019). Shallow ground temperature measurements on the highest volcano on Earth, Mt. Ojos del Salado, Arid Andes, Chile. *Permafrost and Periglacial Processes*, *30*(1), 3–18. https://doi.org/10.1002/ppp.1989
Oeser, R. A., Stroncik, N., Moskwa, L.-M., Bernhard, N., Schaller, M., Canessa, R., et al. (2018). Chemistry and microbiology of the Critical Zone along a steep climate and vegetation gradient in the Chilean Coastal Cordillera. *Catena*, *170*, 183–203. https://doi.org/10.1016/j.catena.2018.06.002
Pfeiffer, M., Padarian, J., Osorio, R., Bustamante, N., Olmedo, G. F., Guevara, M., et al. (2020). CHLSOC. The Chilean Soil Organic Carbon database, a multi-institutional collaborative effort. *Earth System Science Data*, *12*(1), 457–468. https://doi.org/10.5194/essd-12-457-2020
QGIS Development Team. (2017). Version 2.18.13. QGIS geographic information system. Open Source Geospatial Foundation Project. Retrieved from http://qgis.osgeo.org
Ran, Q., Su, D., Li, P., & He, Z. (2012). Experimental study of the impact of rainfall characteristics on runoff generation and soil erosion. *Journal of Hydrology*, *424–425*, 99–111. https://doi.org/10.1016/j.jhydrol.2011.12.035
R Core Team. (2020). R: A language and environment for statistical computing. Version. Retrieved from https://www.R-project.org/
Rech, J. A., Quade, J., & Hart, W. S. (2003). Isotopic evidence for the source of Ca and S in soil gypsum, anhydrite and calcite in the Atacama Desert, Chile. *Geochimica et Cosmochimica Acta*, *67*(4), 575–586. https://doi.org/10.1016/S0016-7037(02)01175-4
Red Cedeus. (2021). By GeoNode (2018) Version 2.0.1. Retrieved from http://datos.cedeus.cl/layers/
Rillig, M. C., Ryo, M., Lehmann, A., Aguilar-Trigueros, C. A., Buchert, S., Wulf, A., et al. (2019). The role of multiple global change factors in driving soil functions and microbial biodiversity. *Science (New York, N.Y.)*, *366*(6467), 886–890. https://doi.org/10.1126/science.aay2832
Seabold, S. & Perktold, J. (2010). statsmodels: Econometric and statistical modeling with python. Version. In 9th Python in Science Conference. Retrieved from https://www.statsmodels.org/stable/index.html
Shen, J., Wyness, A. J., Claire, M. W., & Zerkle, A. L. (2021). Spatial variability of microbial communities and salt distributions across a latitudinal aridity gradient in the Atacama Desert. *Microbial Ecology*, *82*(2), 442–458. https://doi.org/10.1007/s00248-020-01672-w
SigmaPlot. (2008). Systat Software, Inc. Version 11.0.0.75.
Siqueira, R. G., Schaefer, C. E. G. R., Fernandes, F. E. I., Corrêa, G. R., Francelino, M. R., de Souza, J. J. L. L., & Rocha, P. de A. (2021). Weathering and pedogenesis of sediments and basaltic rocks on Vega Island, Antarctic Peninsula. *Geoderma*, *382*(21), 114707. https://doi.org/10.1016/j.geoderma.2020.114707

Slowikowski, K. (2021). *ggrepel: Automatically position non-overlapping text labels with 'ggplot2'. R package version 0.9.1* Retrieved from https://CRAN.R-project.org/package=ggrepel

Sun, T., Bao, H., Reich, M., & Hemming, S. R. (2018). More than ten million years of hyper-aridity recorded in the Atacama Gravels. *Geochimica et Cosmochimica Acta*, *227*, 123–132. https://doi.org/10.1016/j.gca.2018.02.021

Sutter, B., Dalton, J. B., Ewing, S. A., Amundson, R., & McKay, C. P. (2007). Terrestrial analogs for interpretation of infrared spectra from the Martian surface and subsurface. Sulfate, nitrate, carbonate, and phyllosilicate-bearing Atacama Desert soils. *Journal of Geophysical Research*, *112*(G4). https://doi.org/10.1029/2006JG000313

Taylor, L. L., Leake, J. R., Quirk, J., Hardy, K., Banwart, S. A., & Beerling, D. J. (2009). Biological weathering and the long-term carbon cycle. Integrating mycorrhizal evolution and function into the current paradigm. *Geobiology*, *7*(2), 171–191. https://doi.org/10.1111/j.1472-4669.2009.00194.x

Tielbörger, K., Bilton, M. C., Metz, J., Kigel, J., Holzapfel, C., Lebrija-Trejos, E., et al. (2014). Middle-Eastern plant communities tolerate 9 years of drought in a multi-site climate manipulation experiment. *Nature Communications*, *5*, 5102. https://doi.org/10.1038/ncomms6102

Uritskiy, G., Getsin, S., Munn, A., Gomez-Silva, B., Davila, A., Glass, B., et al. (2019). Halophilic microbial community compositional shift after a rare rainfall in the Atacama Desert. *The ISME Journal*, *13*(11), 2737–2749. https://doi.org/10.1038/s41396-019-0468-y

Voigt, C., Klipsch, S., Herwartz, D., Chong, G., & Staubwasser, M. (2020). The spatial distribution of soluble salts in the surface soil of the Atacama Desert and their relationship to hyperaridity. *Global and Planetary Change*, *184*, 103077. https://doi.org/10.1016/j.gloplacha.2019.103077

Warren-Rhodes, K. A., Lee, K. C., Archer, S. D. J., Cabrol, N., Ng-Boyle, L., Wettergreen, D., et al. (2019). Subsurface microbial habitats in an extreme desert Mars-Analog environment. *Frontiers in Microbiology*, *10*, 69. https://doi.org/10.3389/fmicb.2019.00069

Warren-Rhodes, K. A., Rhodes, K. L., Pointing, S. B., Ewing, S. A., Lacap, D. C., Gómez-Silva, B., et al. (2006). Hypolithic cyanobacteria, dry limit of photosynthesis, and microbial ecology in the hyperarid Atacama Desert. *Microbial Ecology*, *52*(3), 389–398. https://doi.org/10.1007/s00248-006-9055-7

Wickham, H. (2016). *ggplot2. Elegant graphics for data analysis*. Cham: Springer (Use R!). https://doi.org/10.1007/978-3-319-24277-4

Zhang, K., Shi, Y., Cui, X., Yue, P., Li, K., Liu, X., et al. (2019). Salinity is a key determinant for soil microbial communities in a desert ecosystem. *mSystems*, *4*(1). https://doi.org/10.1128/mSystems.00225-18